Andrographolide acts with dexamethasone to inhibit the growth of acute lymphoblastic leukemia CEM-C1 cells via the regulation of the autophagy-dependent PI3K/AKT/mTOR signaling pathway

XIAOWEN LI[1*], TONG WU[1*], WEIHONG CHEN[1*], JIANNAN ZHANG[1], YANPING JIANG[2], JIANZHI DENG[3], WENQING LONG[2], XI QIN[4] and YUEHAN ZHOU[1]

[1]Department of Clinical Pharmacy, College of Pharmacy; [2]Department of Clinical Medicine, College of Lingui Clinical Medicine, Guilin Medical University, Guilin, Guangxi Zhuang Autonomous Region 541199; [3]Guangxi Key Laboratory of Embedded Technology and Intelligent System, Guilin University of Technology, Guilin, Guangxi Zhuang Autonomous Region 541004; [4]Department of Medical Oncology, Affiliated Hospital of Guilin Medical University, Guilin, Guangxi Zhuang Autonomous Region 541001, P.R. China

Abstract. Acute lymphoblastic leukemia (ALL) is one of the most common malignant tumor types of the circulatory system. Dexamethasone (DEX) acts on the glucocorticoid (GC) receptor (GR) and is a first-line chemotherapy drug for ALL. However, long-term or high-dose applications of the drug can not only cause adverse reactions, such as osteoporosis and high blood pressure, but can also cause downregulation of GR and lead to drug resistance. In the present study, reverse transcription-quantitative PCR, western blotting and LysoTracker Red staining were used to observe the effects of DEX and andrographolide (AND; a botanical with antitumorigenic properties) combined treatment. It was found that AND enhanced the sensitivity of CEM-C1 cells, a GC-resistant cell line, to DEX, and synergistically upregulated GR both at the transcriptional and post-transcriptional level with DEX. The combination of AND with DEX synergistically alkalized lysosomal lumen and downregulated the expression of autophagy-related genes Beclin1 and microtubule-associated 1 protein light chain 3 (LC3), thereby inhibiting autophagy. Knocking down LC3 expression enhanced GR expression, suggesting that GR was regulated by autophagy. Furthermore, compared with the monotherapy group (AND or DEX in isolation), AND interacted with DEX to activate the autophagy-dependent PI3K/AKT/mTOR signaling pathway by enhancing the phosphorylation of PI3K, AKT and mTOR, thereby decreasing GR degradation and increasing the sensitivity of cells to GCs. In conclusion, the present study demonstrated that AND exhibited a synergistic anti-ALL effect with DEX via upregulation of GR, which was orchestrated by the autophagy-related PI3K/AKT/mTOR signaling pathway. The results of the present study therefore provided novel research avenues and strategies for the treatment of ALL.

Introduction

Acute lymphoblastic leukemia (ALL) is an aggressive type of leukemia characterized by excessive lymphoblasts or lymphocytes in the bone marrow and peripheral blood, which can spread to the lymph nodes, spleen, liver, central nervous system and other organs (1,2). While it predominantly affects children, ALL represents 20% of leukemia cases in adults, of which B cell lineage ALL constitutes 75% (3-5). Over the past decades, treatment-related mortality rates during induction chemotherapy in patients with ALL have decreased due to improved supportive care (6). In addition, the use of risk-directed therapy to optimize doses and schedules of chemotherapy has been developed over the past 40 years (7), which has increased the survival probability to 80-90% (8). Thus, most children with ALL can be cured; however, with increasing age, adult patients have higher white blood cell counts, a lower incidence of hyperdiploidy, an increased incidence of adverse genetic abnormalities, and are at lower biological risk and reduced tolerance to chemotherapy, which leads to poor prognosis in adult patients with ALL (9-11). Clinical studies have demonstrated that chemotherapy remains the most common treatment option (12,13). However, certain studies have reported that, in the treatment

Correspondence to: Professor Yuehan Zhou, Department of Clinical Pharmacy, College of Pharmacy, Guilin Medical University, 1 Zhiyuan Road, Guilin, Guangxi Zhuang Autonomous Region 541199, P.R. China
E-mail: yuehanzhou@glmc.edu.cn

Dr Xi Qin, Department of Medical Oncology, Affiliated Hospital of Guilin Medical University, 15 Lequn Road, Guilin, Guangxi Zhuang Autonomous Region 541001, P.R. China
E-mail: qxglyxy@126.com

*Contributed equally

of ALL, cell resistance is still an important problem in clinical treatment and relapse (14,15).

Glucocorticoids (GCs), including dexamethasone (DEX), are commonly used in ALL chemotherapy (16). GCs function by activating the GC receptor (GR), a ligand-induced transcription factor, which in turn regulates genes that induce leukemic cell apoptosis (17), indicating that GCs serve an important role in the therapy and prognosis of ALL. However, it has been reported that the long-term application of GCs, even at therapeutic doses, can lead to adverse reactions and trigger downregulation of GR, which results in resistance to GCs (18,19). Therefore, inhibiting the downregulation of GR (thereby maintaining the sensitivity of ALL to GCs) is essential for the improvement of ALL treatment (19-22). Thus, the exploration of a more effective combination therapy for ALL has been of interest in recent years. Combination therapy can reduce the dosage of GCs, lessen side effects and improve the therapeutic effect, which is an effective method to reduce chemotherapy resistance in ALL cells (23).

Andrographolide (AND) is the major bioactive compound isolated from *Andrographis paniculata*, a medicinal herb that is widely used in China and other parts of Asia for the treatment of upper respiratory tract infections (24). It has been found that AND has a wide range of therapeutic actions, including immunosuppressant (25), antithrombotic (26), anti-inflammatory (27), antineoplastic (28), antiviral (29,30), antibacterial (31), antidiabetic (30,32), antioxidative (33), antipyretic (34), anti-oedematogenic and antinociceptive activities (35). It has also been reported that AND is a common inhibitor of autophagy (36,37). A previous study reported that AND could inhibit the growth of the ALL cell line Jurkat (38), which provides some evidence for the possible clinical application of AND in ALL.

Autophagy is an essential and conserved lysosomal degradation pathway that controls the homeostasis of the cytoplasm by bulk degradation of unnecessary or dysfunctional cellular organelles and protein aggregates (39). In addition to the previously described tumor-suppressive roles of autophagy, the pro-survival function of autophagy under stress conditions, including nutrient deprivation, hypoxia and therapeutic stress, has been found to promote tumor growth and progression (40,41). In the autophagy process, precursor microtubule-associated 1 protein light chain 3 (LC3) is processed by autophagy-related protein (ATG) 4 into cytoplasmic soluble LC3I, which is then covalently linked to phosphatidylethanolamine (PE), by ATG7 and ATG3, to become lipid-soluble LC3-PE (also known as LC3II), which then participates in membrane elongation until the formation of the autolysosome (42,43). Consequently, LC3II, an important multi-signal transduction regulating protein located on the autophagic vesicular membrane, is often used as a marker of autophagy formation (44). Beclin1 was the first confirmed mammalian autophagy gene and the first gene in the lysosomal degradation pathway of autophagy to be identified as a tumor suppressor (45). Studies have demonstrated that Beclin1 binds to proteins such as vacuolated protein sorting associated protein (VPS) 15, VPS34, UV radiation resistance associated gene product (UVRAG) and ATG14 to form a class III PI3K complex, which controls autophagosome formation and regulates autophagy activity (46,47). In hematologic malignancies,

autophagy can either act as a chemoresistance mechanism or have tumor-suppressive functions (21). When cells undergo lysosomal autophagy, GRs are degraded by lysosomes (48), thereby reducing the sensitivity of ALL cells to drugs. Therefore, we hypothesize that autophagy is important in the resistance of ALL cells and the GR drug receptor to GCs.

The PI3K/AKT/mTOR signaling pathway serves a crucial role in cellular signaling and regulates various cellular functions, including cell growth and death (49,50). Upon entering the cell, PI3K catalyzes the generation of phosphatidylinositol-3,4,5-triphosphate (PIP3), a second messenger, alongside related active enzymes (such as tyrosine kinase and small Ras-related GTPases). PIP3 subsequently activates AKT in conjunction with phosphatidylinositol lipid-dependent protein kinase 1. Activated AKT prevents tuberous sclerosis complex 1/2 complex degradation, promoting mTOR activation and inhibiting cellular autophagy (51). It has been demonstrated that activation of the PI3K/AKT/mTOR signaling pathway can block cellular autophagy to enhance drug sensitivity in tumor therapy (52). Consequently, targeting the PI3K/AKT/mTOR signaling pathway to induce autophagy may increase tumor cell susceptibility to drugs.

Based on the aforementioned studies, the present study aimed to determine the synergistic antitumor effect of AND and DEX on a DEX-resistant ALL cell line (CEM-C1). In terms of autophagy and drug resistance, studying the inhibitory effect of autophagy inhibitors combined with DEX on ALL has important research value.

Materials and methods

Cell culture and drug treatment. The CEM-C1 cells used in the present study were obtained from The Cell Bank of Type Culture Collection of The Chinese Academy of Sciences. CEM-C1 cells were maintained in RPMI-1640 medium (cat. no. C11875500BT; Gibco; Thermo Fisher Scientific, Inc.) with 10% fetal bovine serum (cat. no. S711-001S; Lonsera; Shanghai Shuangru Biotechnology Co., Ltd.) and 1% penicillin-streptomycin (cat. no. sv30010; HyClone; Cytiva). Cells were kept in a humidified atmosphere of 5% CO_2 at 37˚C.

AND (cat. no. 365645; Sigma-Aldrich; Merck KGaA) and DEX (cat. no. A17590;Thermo Fisher Scientific, Inc.) were prepared in DMSO and diluted in culture medium when needed. The final concentration of DMSO was <0.5%, which did not affect cell survival (53). Cells were treated with different concentrations of the drugs: Control group (RPMI-1640 medium without drugs), 5 μM AND, 50 μM DEX or 5 μM AND + 50 μM DEX, and then incubated for 24 h in a humidified atmosphere of 5% CO_2 at 37˚C.

Cell viability assay. CEM-C1 cells were cultured in 96-well plates and seeded at $1x10^4$ cells per well. After 24 h, different concentrations of drugs were added and the cells were incubated for a further 24 h in a humidified atmosphere of 5% CO_2 at 37˚C. The cell treatment groups were as follows: i) Untreated control group (control), RPMI-1640 medium without drugs; ii) solvent control group (vehicle), 0.1% DMSO (the same concentration used at the highest dose of AND); iii) AND only group, AND was added at concentrations of 1.25, 2.5, 5, 10, 20 or 40 μM; iv) DEX group, DEX was added at concentrations

of 12.5, 25, 50, 100, 200 or 400 μM; and v) co-treatment group, AND and DEX were added at various concentrations (1.25 μM AND + 12.5 μM DEX, 2.5 μM AND + 25 μM DEX, 5 μM AND + 50 μM DEX or 10 μM AND + 100 μM DEX). After treatment, the cell viability was measured using a Cell Counting Kit-8 (CCK-8; cat. no. CK04; Dojindo Laboratories, Inc.) assay: CCK-8 (10 μl) was added to each well in the dark and incubated for 4 h. The optical density was measured with a microplate reader (Bio-Rad Laboratories, Inc.) at a wavelength of 450 nm. The survival rate of the drug-treated groups was compared with that of the untreated control group.

Calculation of the combined effect of AND and DEX. CompuSyn software (version 1.0; ComboSyn, Inc.) was used to calculate the combination index (CI) (54). If the CI was <1, the combined effect was considered synergistic; if CI=1, the effect of the two drugs was considered to be additive; and if the CI was >1, the combined effect was considered to be antagonistic.

Wright-Giemsa staining. The CEM-C1 cells were cultured in 6-well plates at 1×10^6 cells per well. After the aforementioned drug treatment, cells were washed with PBS three times and suspended in 0.5 ml PBS per well. The smear slides were constructed slowly with 15 μl cell suspension, then fixed with 4% paraformaldehyde (cat. no. P1110; Beijing Solarbio Science & Technology Co., Ltd.) at room temperature for 30 min. Following this, the cells were washed three times with PBS. The slides were then dried and stained by Wright-Giemsa (cat. no. G1020; Beijing Solarbio Science & Technology Co., Ltd.) staining at room temperature, according to the manufacturer's instructions. The slides were then washed with PBS, dried and observed under a light microscope (Olympus Corporation). The quantification of stained cells was performed using ImageJ software (version 4.1; National Institutes of Health).

Reverse transcription-quantitative PCR (RT-qPCR). After the aforementioned drug treatments in a 6-well plate, total RNA in the treated cells was isolated using TRIzol® (Invitrogen; Thermo Fisher Scientific, Inc.). RNA was reverse transcribed into cDNA using the RevertAid First Strand cDNA Synthesis Kit (Thermo Fisher Scientific, Inc.). The temperature protocol for the RT was as follows: 25°C for 5 min, 42°C for 60 min and 70°C for 5 min. GR, LC3 and Beclin1 were detected by qPCR using the SYBR Green Kit (Shanghai Yeasen Biotechnology Co., Ltd.). The amplification parameters were as follows: 95°C for 10 min, followed by 40 cycles of 95°C for 10 sec, 60°C for 20 sec and 72°C for 20 sec. The primer sequences used were as follows: GR forward, 5'-AGGACCACCTCCCAA ACTCT-3' and reverse, 5'-TGTTTTTCGAGCTTCCAGGT-3'; LC3 forward, 5'-CCGACTTATTCGAGAGCAGCATCC-3' and reverse, 5'-GTCCGTTCACCAACAGGAAGAAGG-3'; Beclin1 forward, 5'-ATCTAAGGAGCTGCCGTTATAC-3' and reverse, 5'-CTCCTCAGAGTTAAACTGGGTT-3'; and GAPDH forward, 5'-CAGGAGGCATTGCTGATGAT-3' and reverse, 5'-GAAGGCTGGGGCTCATTT-3'. The primers were designed and synthetized by Sangon Biotech Co., Ltd. Expression was analyzed using the $2^{-\Delta\Delta Cq}$ method (55) with GAPDH as the reference gene. All experiments were conducted in triplicate.

Western blotting. Western blotting experiments were conducted as previously described (53). The drug-treated cells were lysed at 4°C in RIPA buffer (Thermo Fisher Scientific, Inc.), which contained protease and phosphatase inhibitors (Roche Diagnostics GmbH). The supernatant was collected for protein determination using a BCA protein assay kit (Epizyme, Inc.; Ipsen Biopharmaceuticals, Inc.). An equal amount of protein (30 μg/lane) was resolved via 8, 10 or 15% SDS-PAGE, and separated proteins were then transferred to a PVDF membrane. The membranes were blocked with 5% non-fat milk (Beijing Solarbio Science & Technology Co., Ltd.) in tris-buffered saline containing 0.1% Tween-20 for 2 h at room temperature, and then incubated with primary antibodies (1:1,000) overnight at 4°C. The antibodies used in the present study were: GR (cat. no. 3660S), LC3II/LC3I (cat. no. 12741), Beclin1 (cat. no. 3495S), PI3K (cat. no. 4257S), phosphorylated (p-)PI3K (cat. no. 4228S), AKT (cat. no. 4691S), p-AKT (cat. no. 4060S), mTOR (cat. no. 2983S), p-mTOR (cat. no. 5536S) (all purchased from Cell Signaling Technology, Inc.), GAPDH (cat. no. AF0006) and β-actin (cat. no. AF0003) (all purchased from Beyotime Institute of Biotechnology). The membranes were then incubated with horseradish peroxidase-labeled secondary antibodies [anti-mouse IgG (1:2,000; cat. no. 7076; Cell Signaling Technology, Inc.) and anti-rabbit IgG (1:2,000; cat. no. 7074; Cell Signaling Technology, Inc.)] for 2 h at room temperature. The immunoreactive bands were visualized using an ECL western blot detection kit (Epizyme, Inc.; Ipsen Biopharmaceuticals, Inc.) and a Tanon 5200 Imaging System (Tanon Science and Technology Co., Ltd.). The intensity of the immunoblotting bands was measured using ImageJ software.

LysoTracker Red staining. After the aforementioned drug treatment in 6-well plates, cells were stained with LysoTracker Red (50 nM), a specific red fluorescent dye for lysosomes, for 45 min at 37°C, followed by counterstaining with Hoechst 33342 for 15 min at room temperature in the dark. The cells were then observed and imaged using an inverted fluorescence microscope (Olympus Corporation).

Small interfering RNA (siRNA) and transfection. The siRNA experiments were divided into five groups: The control (untreated control group, RPMI-1640 medium only), 50 nM negative control (NC; non-targeting sequence; cat. no. siN0000001-1-5), 50 nM positive control (PC; h-ACTB; siP0000002-1-5), si-LC3-1, si-LC3-2 and si-LC3-3 (all 50 nM) groups. The si-LC3 and NC sequences were designed and synthesized by Guangzhou RiboBio Co., Ltd. The si-LC3 nucleotide sequences used were as follows: si-LC3-1, 5'-ATTCCTGTACATGGT CTAT-3'; si-LC3-2, 5'-TATGCCTCCCAGGAGACGT-3'; and si-LC3-3, 5'-GATTCCTGTACATGGTCTA-3'. For transfection, cells were seeded into a 6-well plate at a density of 5×10^5 cells per well. When the cell density reached 70-80%, 250 μl transfection complex solution was added, which was prepared following the instructions of the siRNA reagent kit (Guangzhou RiboBio Co., Ltd.) and Lipofectamine® 3000 reagent (Thermo Fisher Scientific, Inc.). In brief, solution A (5 μl 20 μM siRNA stock solution + 120 μl RPMI-1640) was mixed with solution B (3.5 μl Lipofectamine 3000 + 125 μl RPMI-1640) and incubated for 20 min at room temperature to form the transfection complex solution. Cells were kept in a humidified atmosphere of 5% CO_2 at 37°C for 24 h. After 24 h of transfection, total cellular proteins
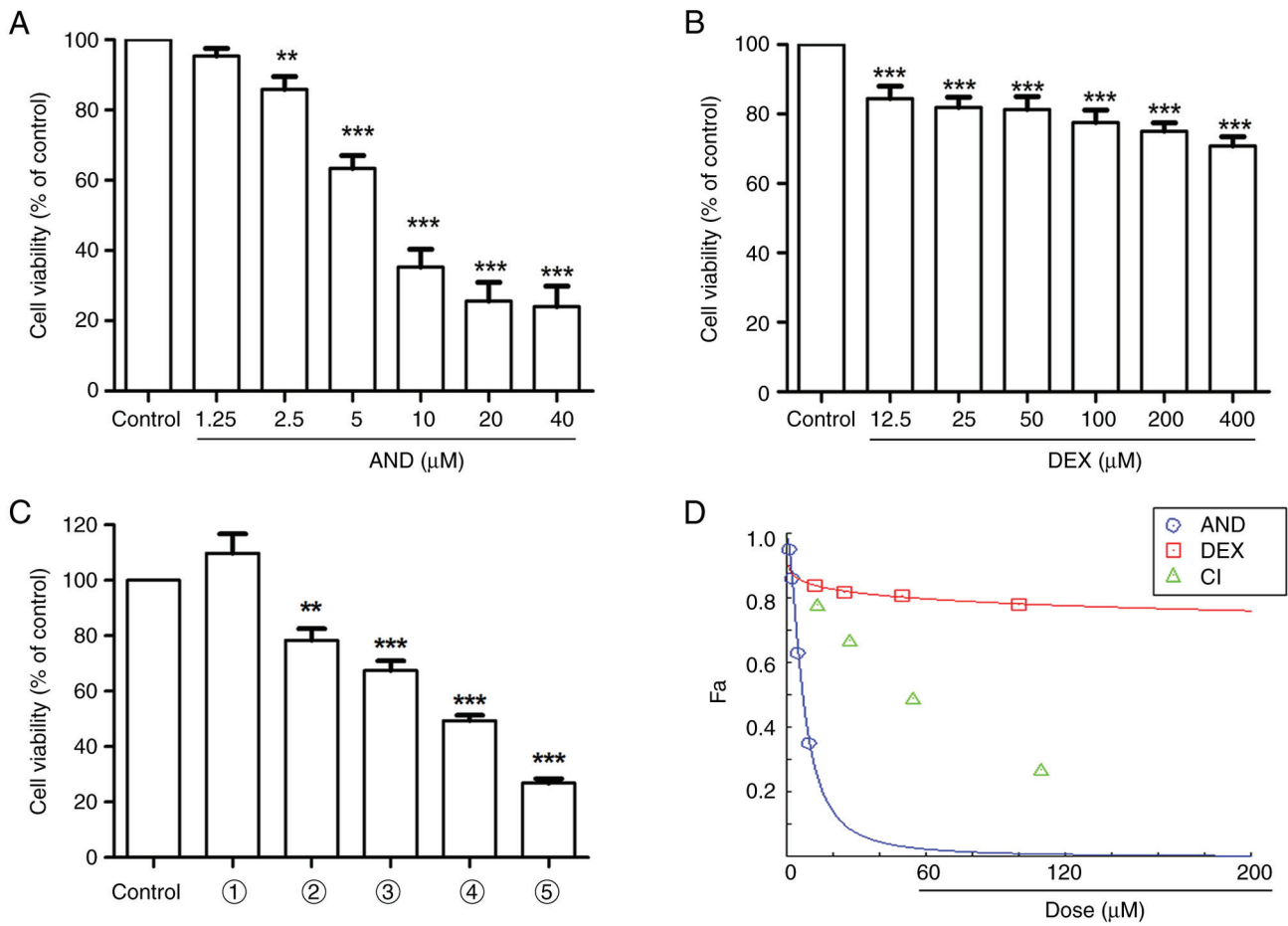
Figure 1. Effect of AND, DEX or AND + DEX on the viability of CEM-C1 cells. Viability of CEM-C1 cells following (A) AND or (B) DEX treatment, measured using a CCK-8 assay. (C) Effect of AND + DEX on CEM-C1 cell viability, measured using a CCK-8 assay. 1, vehicle; 2, 1.25 μM AND + 12.5 μM DEX; 3, 2.5 μM AND + 25 μM DEX; 4, 5 μM AND + 50 μM DEX; and 5, 10 μM AND + 100 μM DEX. (D) CompuSyn software was used to analyze the CI presented in (C). n=3; **P<0.01, ***P<0.001 vs. control. AND, andrographolide; CCK-8, Cell Counting Kit-8; CI, combination index; DEX, dexamethasone; Fa, fraction affected.

were extracted and the transfection efficiency was analyzed by western blotting as aforementioned.

Statistical analysis. Statistical analyses were conducted using SPSS 25.0 (IBM Corp.). All data are presented as the mean ± standard deviation and all experiments were repeated three times. Differences among groups were analyzed using one-way ANOVA, followed by Tukey's post hoc test for multiple comparisons. P<0.05 was considered to indicate a statistically significant difference.

Results

Co-treatment with AND + DEX inhibits the viability of CEM-C1 cells. As shown in Fig. 1A-C, compared with the control group, the viability of the cells incubated with AND, DEX or AND + DEX decreased with increasing drug concentrations. According to Fig. 1D, the CI values were all <1, indicating that the combination of the two drugs had a synergistic effect.

Wright-Giemsa staining indicates alterations of the cell morphology. According to the results of the Wright-Giemsa staining (Fig. 2), compared with the administration of 5 μM AND or 50 μM DEX groups, the CEM-C1 cells were smaller

in the AND + DEX group (Fig. 2F). In addition, the cells were uniformly stained to purple and the number of stained cells was reduced in the AND + DEX group (Fig. 2E). These results indicated that, compared with the AND or DEX groups, co-treatment with 5 μM AND + 50 μM DEX had a greater inhibitory effect on the growth of CEM-C1 cells.

Co-treatment with AND + DEX upregulates GR expression. GR mRNA expression in CEM-C1 cells following drug treatment was detected via RT-qPCR. As shown in Fig. 3A, compared with that in the control group, GR expression was significantly increased in the DEX and AND + DEX groups, and GR expression in the AND + DEX group was higher than that in the DEX group. Subsequently, changes in GR protein expression were analyzed by western blotting, which further confirmed that GR expression in CEM-C1 cells of the AND + DEX group was significantly upregulated compared with that in the control and DEX groups (Fig. 3B and C). The aforementioned results suggested that the combination of the two drugs upregulated the transcription and post-transcription levels of GR.

Co-treatment with AND + DEX alkalizes the lysosomal lumen. LysoTracker Red is sensitive to pH alteration and can be used to label and track acidic organelles (such as autolysosomes)
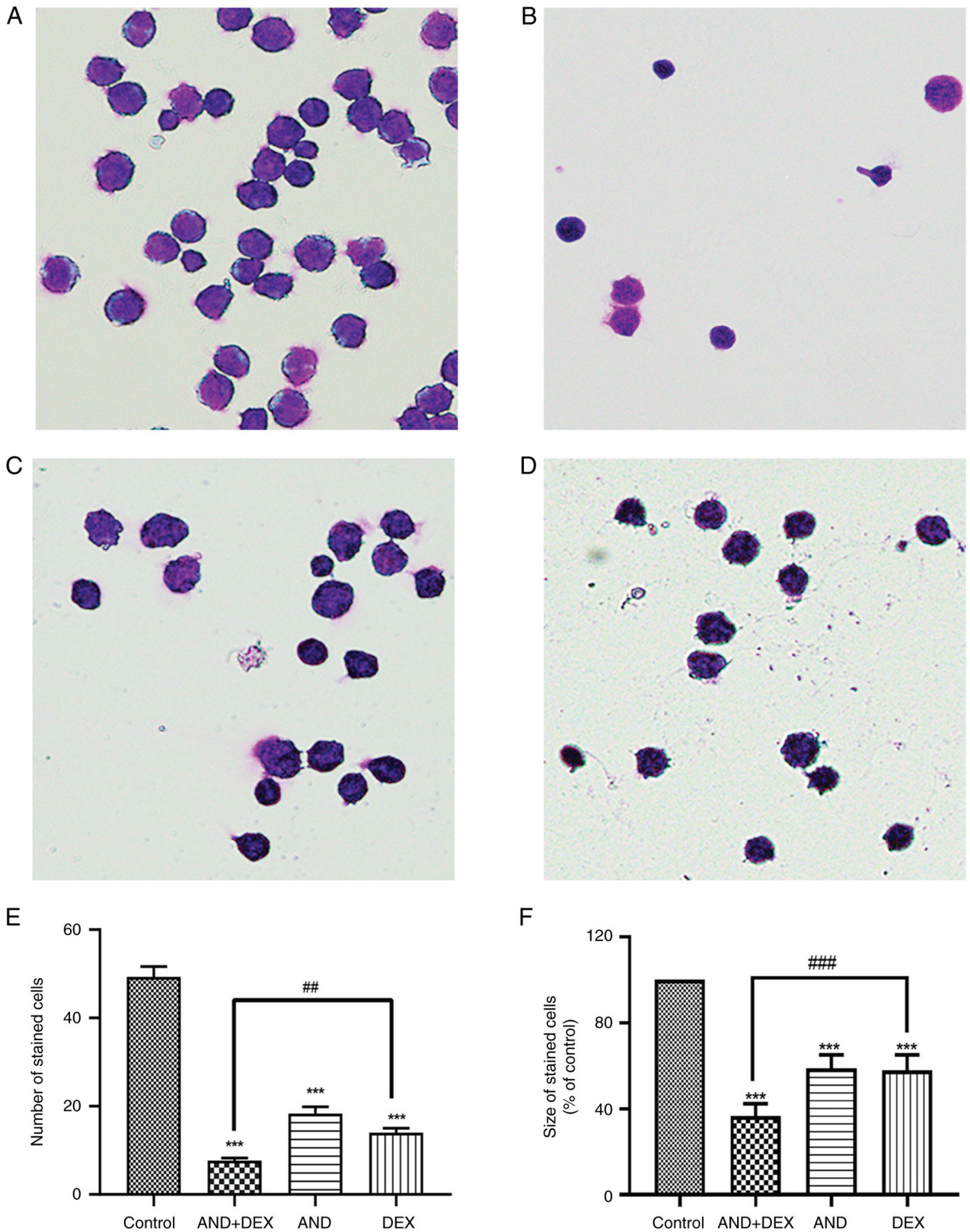
Figure 2. Wright-Giemsa staining to detect the effect of AND, DEX or AND + DEX on the morphology of CEM-C1 cells. Wright-Giemsa staining of (A) the blank control group, and the (B) 5 μM AND + 50 μM DEX, (C) 5 μM AND and (D) 50 μM DEX groups (magnification, x400). Quantification of the (E) number and the (F) size of cells stained following Wright-Giemsa staining. n=3. ***P<0.001 vs. control; ##P<0.01 vs. DEX only. AND, andrographolide; DEX, dexamethasone.

in live cells. The fluorescence intensity of LysoTracker Red has a negative correlation with the pH of the lysosome (56). As shown in Fig. 4A, the nucleus of CEM-C1 cells exhibited

blue fluorescence following incubation with Hoechst 33342 and the cells exhibited red fluorescence following staining with LysoTracker Red. Compared with that of the 50 μM DEX group,
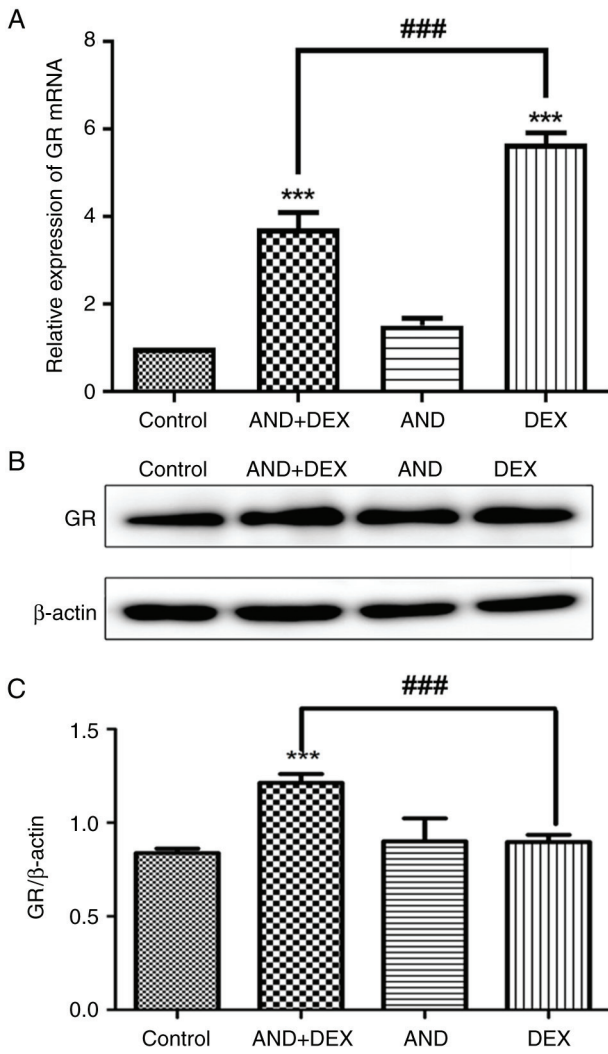
Figure 3. Effect of AND (5 μM), DEX (50 μM) or AND (5 μM) + DEX (50 μM) on GR expression. (A) Reverse transcription-quantitative PCR was used to detect GR expression. GAPDH was used as the internal reference. (B) Western blot images and (C) semi-quantification of GR expression. n=3. ***P<0.001 vs. control; ###P<0.001 vs. DEX only. AND, andrographolide; DEX, dexamethasone; GR, glucocorticoid receptor.

Figure 4. Effect of AND (5 μM), DEX (50 μM) or AND (5 μM) + DEX (50 μM) on the lysosomal pH of CEM-C1 cells. (A) Hoechst 33342 was used to label the nuclei and LysoTracker Red was used to label the lysosomes (magnification, x200). (B) Quantification of the fluorescence intensity of cells stained following LysoTracker staining. AND, andrographolide; DEX, dexamethasone.

the LysoTracker Red fluorescence intensity of the AND + DEX group was significantly reduced (Fig. 4B), which suggested that the lysosomal lumen of CEM-C1 cells was alkalized and the lysosomal pH was increased by co-treatment with AND + DEX.

Co-treatment with AND + DEX inhibits the expression of autophagy-related genes. The mRNA expression levels of Beclin1 and LC3 in CEM-C1 cells following treatment were determined by RT-qPCR. As shown in Fig. 5A, compared with that in the control group, Beclin1 mRNA expression was significantly increased in the DEX and AND + DEX groups, and the level in the combination group was lower than that in the DEX group. Similarly, LC3 mRNA expression was significantly decreased in the drug-treated groups, and the LC3 mRNA expression in the AND + DEX group was lower than that in the DEX group (Fig. 5B). The changes in Beclin1 and LC3 protein expression were subsequently examined via western blotting. As shown in Fig. 5C and E, the protein expression levels of Beclin1 in the AND + DEX group were reduced compared with those in
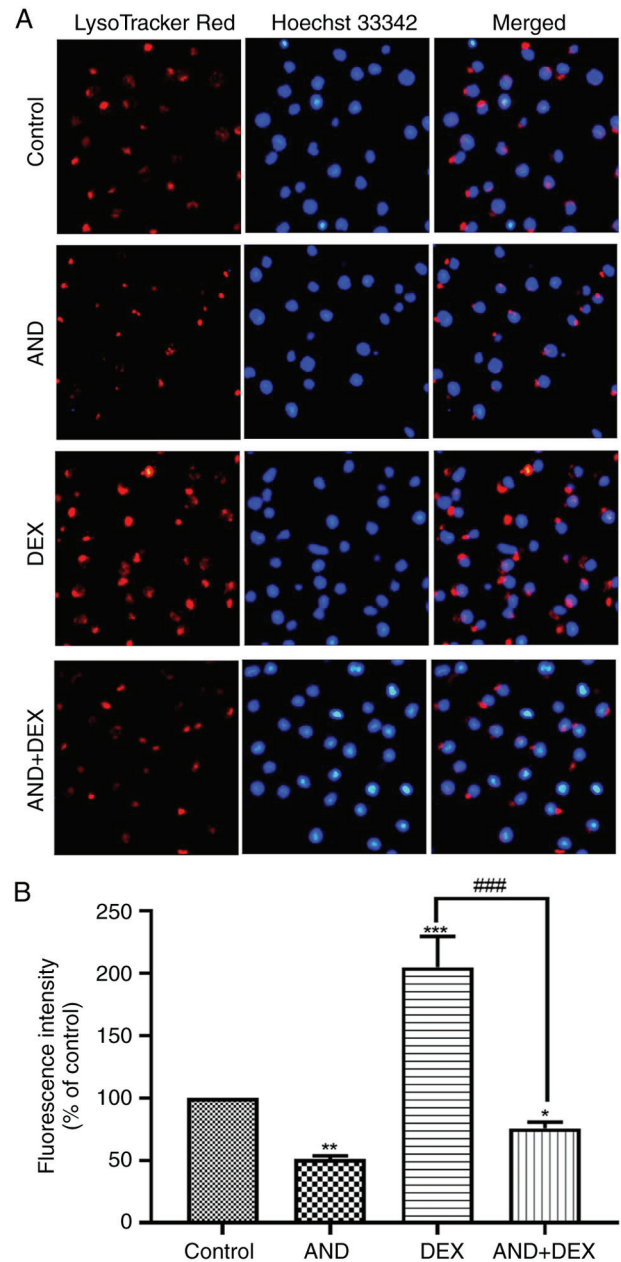
the control and 50 μM DEX groups. Additionally, as shown in Fig. 5D and F, compared with the 50 μM DEX group, the conversion of LC3I to LC3II was reduced and the protein expression levels of LC3II/LC3I were downregulated in the AND + DEX group. These results indicated that the combination of these two drugs regulated the transcription and post-transcriptional levels of autophagy-related genes.

Co-treatment with AND + DEX alters the PI3K/AKT/mTOR signaling pathway in CEM-C1 cells. Western blotting was conducted to detect the expression levels of key proteins in the PI3K/AKT/mTOR signaling pathway. As shown in
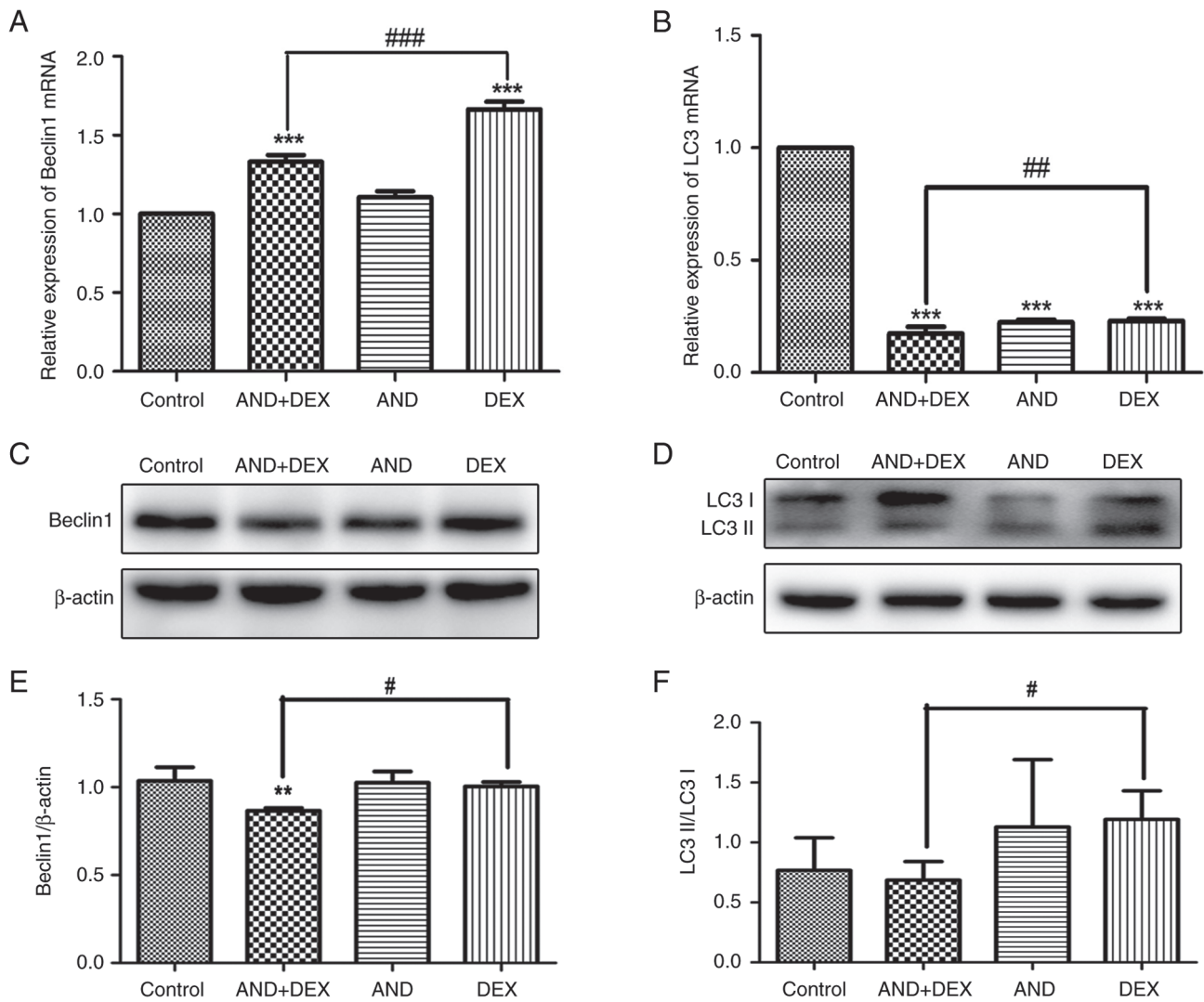
Figure 5. Effect of AND (5 μM), DEX (50 μM) or AND (5 μM) + DEX (50 μM) on autophagy-related gene expression. Reverse transcription-quantitative PCR was used to detect the mRNA expression levels of (A) Beclin1 and (B) LC3. GAPDH was used as the internal reference. (C) Western blot images of Beclin 1 protein expression. (D) Western blot images of LC3I and II expression. (E) Semi-quantification of Beclin protein expression. (F) Semi-quantitation of the ratio of LC3II to LC3I. n=3; **P<0.01, ***P<0.001 vs. control; #P<0.05, ##P<0.01, ###P<0.001 vs. DEX only. AND, andrographolide; DEX, dexamethasone; LC3, microtubule-associated 1 protein light chain 3.

Fig. 6A-D, the levels of p-PI3K, p-AKT and p-mTOR were significantly upregulated in the AND + DEX group compared with the control group. However, the expression levels of total PI3K, AKT and mTOR were not affected (Fig. 6A), indicating that AND acts with DEX to alter the activation of the aforementioned proteins, thus inhibiting autophagy.

GR expression increases following knockdown of the autophagy-related gene, LC3. As shown in Fig. 6E, compared with the control group, β-actin expression was downregulated by PC siRNA transfection at 50 and 100 nM, which did not affect the expression of GAPDH, indicating that PC siRNA successfully knocked down β-actin expression and that the transfection conditions tested were suitable for subsequent experiments. Moreover, since the initial transfection concentration recommended by the manufacturer was also 50 nM, 50 nM was selected for subsequent experiments. In Fig. 6F and G, compared with those in the NC group, the expression levels of LC3 in CEM-C1 cells transfected with si-LC3-1, si-LC3-2 and

si-LC3-3 were decreased, indicating that LC3 knockdown was successful. It was also demonstrated that the knockdown effect of si-LC3-1 was the greatest. Therefore, si-LC3-1 was selected for subsequent experiments. GR expression after knockdown of LC3 expression was subsequently detected by RT-qPCR and western blotting. As shown in Fig. 6H-J, compared with that in the control group, GR mRNA and protein expression was increased following knockdown of LC3 expression, and the difference was statistically significant.

Discussion

The issue of determining prognosis in relapsed patients with ALL has been a persistent concern, with drug-resistant ALL phenotypes being the most prominent biological feature of relapse (57). Combination therapy has been proposed as a potential strategy to overcome this issue (22,23,58,59). In current clinical practice, combination therapy for cancer can reduce drug toxicity and avoid the occurrence of rapid drug resistance (60-62). A
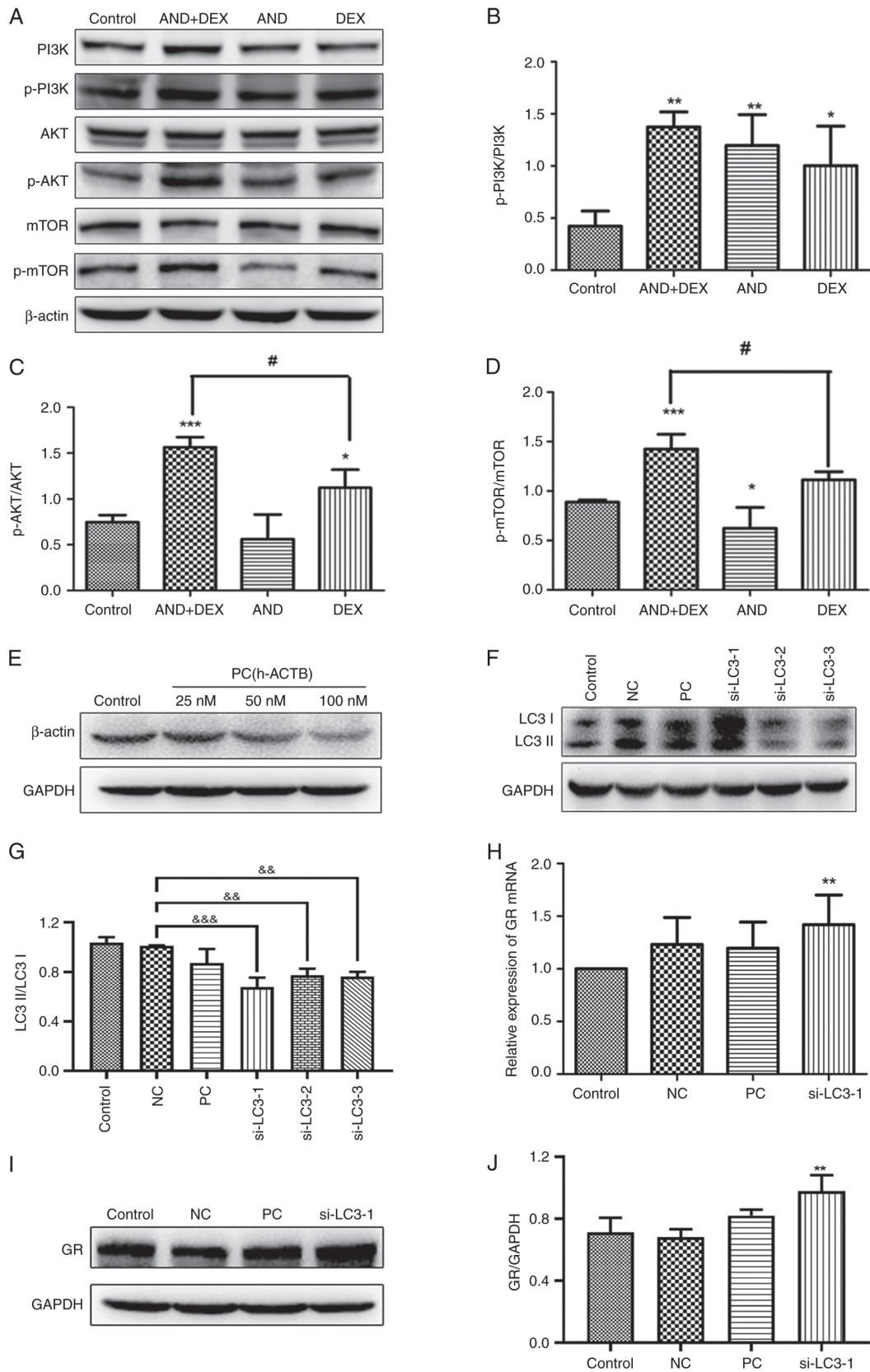
Figure 6. Effect of AND (5 μM), DEX (50 μM) or AND (5 μM) + DEX (50 μM) on the PI3K/AKT/mTOR signaling pathway, and GR expression after knockdown of the autophagy-related gene, LC3. (A) Western blot images of proteins from the PI3K-AKT-mTOR signaling pathway after drug treatment of CEM-C1 cells. The mean ratio of (B) p-PI3K/PI3K, (C) p-AKT/AKT and (D) p-mTOR/mTOR following the densitometric semi-quantification of bands. (E) Transfection efficiency of the PC was determined by western blotting. (F) Transfection efficiency of si-LC3 was determined by western blotting, followed by the (G) semi-quantitation of the ratio of LC3II to LC3I. (H) Reverse transcription-quantitative PCR was used to detect GR mRNA expression following knockdown of LC3. GAPDH was used as the internal reference. (I) Western blot images and (J) semi-quantification of GR protein expression following knockdown of LC3. n=3. *P<0.05, **P<0.01, ***P<0.001 vs. control; #P<0.05 vs. DEX only; &&P<0.01, &&&P<0.001 vs. NC. AND, andrographolide; DEX, dexamethasone; GR, glucocorticoid receptor; LC3, microtubule-associated 1 protein light chain 3; NC, negative control; p-, phosphorylated; PC, positive control; si, small interfering RNA.

previous study has shown that single-agent chemotherapy can trigger autophagy, and the presence of autophagy may induce the multi-drug resistance mechanism of cancer cells (63). It has been reported that AND is a common autophagy inhibitor, and the present study demonstrated that the intensity of the LysoTracker Red fluorescence was attenuated in the AND group compared with the DEX group, suggesting that AND can inhibit autophagy by alkalizing the lysosomal lumen (36,37). In the present study, the combination of 5 μM AND + 50 μM DEX was used to inhibit ALL cell viability. The results of the CCK-8 assay demonstrated that the inhibition rate was as high as 51% in the 5 μM AND + 50 μM DEX group, and the CI indicated that the combination of the two drugs had a synergistic effect. The results of the present study also demonstrated that GR expression was upregulated at the mRNA and protein levels in the AND + DEX group compared with the 50 μM DEX group, which indicated that the combination of the two drugs could increase the transcription of GR and inhibit the degradation of GR protein. These findings, in combination with the aforementioned findings, demonstrated that the mechanism behind GR upregulation by the combination of these two drugs warrants further study.

Autophagy is an evolutionarily conserved process that serves an important role in tumor cell resistance to chemotherapy, and changes in autophagy-related gene expression may contribute to GC resistance in ALL (64). Beclin1, an essential protein for autophagy, transitions from its metastable homodimeric state to interact with key modulators, such as ATG14L or UVRAG, and form functionally distinct ATG14L or UVRAG-containing Beclin1-VPS34 subcomplexes. The Beclin1-VPS34 complex serves essential roles in membrane-mediated transport processes, including autophagy and endosomal trafficking (65,66). In coordination with the Unc-51-like autophagy activating kinase 1 complex, the Beclin1 complex regulates early events in the initiation of autophagosome formation (67,68). Another crucial autophagy protein, LC3B (also known as ATG8F), facilitates autophagosome elongation and maturation, leading to the sequestration of autophagic cargoes (69). The results of the present study demonstrated that the expression levels of LC3II/LC3I and Beclin1 were significantly reduced following the co-treatment with AND + DEX, compared with DEX alone. In addition, GR expression was upregulated following AND + DEX treatment and following knockdown of LC3 expression by siRNA transfection, indicating that treatment with AND + DEX reduced the degradation of GR by inhibiting autophagy. Therefore, AND + DEX combination therapy may serve an anticancer role. In tumor cells, autophagy is regulated by multiple signaling pathways (70), including the PI3K/AKT/mTOR signaling pathway. The PI3K/AKT/mTOR signaling pathway is widely recognized as a fundamental intracellular signaling pathway that plays a role in cell physiology, cancer cell metastasis and tumorigenesis, and inhibits autophagy when activated (71,72). The present study demonstrated that, compared with the control group, the p-PI3K, p-AKT and p-mTOR protein levels were significantly upregulated in the AND + DEX group, further indicating that this treatment combination could inhibit autophagy by activating the PI3K/AKT/mTOR signaling pathway.

In summary, in the present study, AND was found to upregulate transcriptional and post-transcriptional GR expression by inhibiting autophagy and the autophagy-dependent PI3K/AKT/mTOR signaling pathway, thus increasing the sensitivity of drug-resistant cells and serving an anti-ALL role. Therefore, the present study provided a theoretical basis for a novel treatment for ALL, and the presented results warrant further study.

Availability of data and materials

The datasets used and/or analyzed during the current study are available from the corresponding author on reasonable request.

Authors' contributions

YZ and XQ designed the study. XL, TW, WC and JZ conducted experiments. JD, YJ and WL contributed new reagents and analytic tools. XL, JZ, YJ and WL contributed to acquisition of data. XL, TW, JD and XQ performed data analysis. YZ, XL, TW and WC wrote or contributed to the writing of the manuscript. XL and TW confirm the authenticity of all the raw data. All authors read and approved the final version of the manuscript.

Ethics approval and consent to participate

Not applicable.

Patient consent for publication

Not applicable.

Competing interests

The authors are named inventors on Chinese patent, ZL202010550895.1, entitled 'The application of the combination of andrographolide and dexamethasone in the preparation of compound anti-acute lymphoblastic leukemia drugs' held by Guilin Medical University (Guilin, China) for the combination of andrographolide and dexamethasone as a treatment for acute lymphoblastic leukemia, which was approved on April 13, 2021.

References

1. Olivas-Aguirre M, Torres-López L, Pottosin I and Dobrovinskaya O: Overcoming glucocorticoid resistance in acute lymphoblastic leukemia: repurposed drugs can improve the protocol. Front Oncol 11: 617937, 2021.
2. Gregory S: Adult acute lymphoblastic leukemia: treatment and management updates. Semin Oncol Nurs 35: 150951, 2019.
3. Koh WJ, Greer BE, Abu-Rustum NR, Campos SM, Cho KR, Chon HS, Chu C, Cohn D, Crispens MA, Dizon DS, et al: Vulvar cancer, version 1.2017, NCCN clinical practice guidelines in oncology. J Natl Compr Canc Netw 15: 92-120, 2017.
4. Huang FL, Yu SJ and Li CL: Role of autophagy and apoptosis in acute lymphoblastic leukemia. Cancer Control 28: 10732748211019138, 2021.

5. Chennamadhavuni A, Lyengar V, Mukkamalla SKR and Shimanovsky A: Leukemia. In: StatPearls [Internet]. Treasure Island (FL): StatPearls Publishing, 2023.

6. Park H, Youk J, Shin DY, Hong J, Kim I, Kim NJ, Lee JO, Bang SM, Yoon SS, Park WB and Koh Y: Micafungin prophylaxis for acute leukemia patients undergoing induction chemotherapy. BMC Cancer 19: 358, 2019.

7. Rafei H, Kantarjian HM and Jabbour EJ: Recent advances in the treatment of acute lymphoblastic leukemia. Leuk Lymphoma 60: 2606-2621, 2019.

8. Kato M and Manabe A: Treatment and biology of pediatric acute lymphoblastic leukemia. Pediatr Int 60: 4-12, 2018.

9. Martinelli G, Papayannidis C, Piciocchi A, Robustelli V, Soverini S, Terragna C, Marconi G, Lemoli RM, Guolo F, Fornaro A, et al: INCB84344-201: Ponatinib and steroids in frontline therapy for unfit patients with Ph+ acute lymphoblastic leukemia. Blood Adv 6: 1742-1753, 2022.

10. Imai K: Acute lymphoblastic leukemia: Pathophysiology and current therapy. Rinsho Ketsueki 58: 460-470, 2017 (In Japanese).

11. Aureli A, Marziani B, Venditti A, Sconocchia T and Sconocchia G: Acute lymphoblastic leukemia immunotherapy treatment: Now, next, and beyond. Cancers (Basel) 15: 3346, 2023.

12. Lato MW, Przysucha A, Grosman S, Zawitkowska J and Lejman M: The new therapeutic strategies in pediatric T-cell acute lymphoblastic leukemia. Int J Mol Sci 22: 4502, 2021.

13. Guo XM, Fang YJ, Lv CL, Wang YR and Sun XY: Changes of peripheral blood marrow-derived suppressor cell level after chemotherapy induction remission by VDLP regimen and their relationship with immune system in B-ALL children. Zhongguo Shi Yan Xue Ye Xue Za Zhi 25: 1611-1614, 2017 (In Chinese).

14. Follini E, Marchesini M and Roti G: Strategies to overcome resistance mechanisms in T-cell acute lymphoblastic leukemia. Int J Mol Sci 20: 3021, 2019.

15. Samii B, Jafarian A, Rabbani M, Zolfaghari B, Rahgozar S and Pouraboutaleb E: The effects of Astragalus polysaccharides, tragacanthin, and bassorin on methotrexate-resistant acute lymphoblastic leukemia. Res Pharm Sci 18: 381-391, 2023.

16. Inaba H and Pui CH: Glucocorticoid use in acute lymphoblastic leukaemia. Lancet Oncol 11: 1096-1106, 2010.

17. Kruth KA, Fang M, Shelton DN, Abu-Halawa O, Mahling R, Yang H, Weissman JS, Loh ML, Müschen M, Tasian SK, et al: Suppression of B-cell development genes is key to glucocorticoid efficacy in treatment of acute lymphoblastic leukemia. Blood 129: 3000-3008, 2017.

18. Bedewy AM, El-Maghraby SM, Kandil NS and El-Bendary WR: The prognostic value of glucocorticoid receptors for adult acute lymphoblastic leukemia. Blood Res 50: 235-241, 2015.

19. Xu JY and Luo JM: Association between BIM gene and glucocorticoid resistance in children with acute lymphoblastic leukemia. Zhongguo Dang Dai Er Ke Za Zhi 19: 945-949, 2017 (In Chinese).

20. Gong H, Liu L, Cui L, Ma H and Shen L: ALKBH5-mediated m6A-demethylation of USP1 regulated T-cell acute lympho-blastic leukemia cell glucocorticoid resistance by Aurora B. Mol Carcinog 60: 644-657, 2021.

21. Yuan N, Song L, Zhang S, Lin W, Cao Y, Xu F, Fang Y, Wang Z, Zhang H, Li X, et al: Bafilomycin A1 targets both autophagy and apoptosis pathways in pediatric B-cell acute lymphoblastic leukemia. Haematologica 100: 345-356, 2015.

22. Wandler AM, Huang BJ, Craig JW, Hayes K, Yan H, Meyer LK, Scacchetti A, Monsalve G, Dail M, Li Q, et al: Loss of gluco-corticoid receptor expression mediates in vivo dexamethasone resistance in T-cell acute lymphoblastic leukemia. Leukemia 34: 2025-2037, 2020.

23. Kaveh K, Takahashi Y, Farrar MA, Storme G, Guido M, Piepenburg J, Penning J, Foo J, Leder KZ and Hui SK: Combination therapeutics of Nilotinib and radiation in acute lymphoblastic leukemia as an effective method against drug-resistance. PLoS Comput Biol 13: e1005482, 2017.

24. Burgos RA, Alarcón P, Quiroga J, Manosalva C and Hancke J: Andrographolide, an anti-inflammatory multitarget drug: All roads lead to cellular metabolism. Molecules 26: 5, 2020.

25. Guo BJ, Liu Z, Ding MY, Li F, Jing M, Xu LP, Wang YQ, Zhang ZJ, Wang Y, Wang D, et al: Andrographolide derivative ameliorates dextran sulfate sodium-induced experimental colitis in mice. Biochem Pharmacol 163: 416-424, 2019.

26. Li X, Yuan K, Zhu Q, Lu Q, Jiang H, Zhu M, Huang G and Xu A: Andrographolide ameliorates rheumatoid arthritis by regulating the apoptosis-NETosis balance of neutrophils. Int J Mol Sci 20: 5035, 2019.

27. Ahmed S, Kwatra M, Ranjan Panda S, Murty USN and Naidu VGM: Andrographolide suppresses NLRP3 inflammasome activation in microglia through induction of parkin-mediated mitophagy in in-vitro and in-vivo models of Parkinson disease. Brain Behav Immun 91: 142-158, 2021.

28. Doi H, Matsui T, Dijkstra JM, Ogasawara A, Higashimoto Y, Imamura S, Ohye T, Takematsu H, Katsuda I and Akiyama H: Andrographolide, isolated from Andrographis paniculata, induces apoptosis in monocytic leukemia and multiple myeloma cells via augmentation of reactive oxygen species production. F1000Res 10: 542, 2021.

29. Latif R and Wang CY: Andrographolide as a potent and prom-ising antiviral agent. Chin J Nat Med 18: 760-769, 2020.

30. Adiguna SP, Panggabean JA, Atikana A, Untari F, Izzati F, Bayu A, Rosyidah A, Rahmawati SI and Putra MY: Antiviral activities of andrographolide and its derivatives: Mechanism of action and delivery system. Pharmaceuticals (Basel) 14: 1102, 2021.

31. Zhang L, Bao M, Liu B, Zhao H, Zhang Y, Ji X, Zhao N, Zhang C, He X, Yi J, et al: Effect of andrographolide and its analogs on bacterial infection: A review. Pharmacology 105: 123-134, 2020.

32. Kumar G, Singh D, Tali JA, Dheer D and Shankar R: Andrographolide: Chemical modification and its effect on biological activities. Bioorg Chem 95: 103511, 2020.

33. Mussard E, Cesaro A, Lespessailles E, Legrain B, Berteina-Raboin S and Toumi H: Andrographolide, a natural antioxidant: An update. Antioxidants (Basel) 8: 571, 2019.

34. Jadhav AK and Karuppayil SM: Andrographis paniculata (Burm. F) wall ex nees: Antiviral properties. Phytother Res 35: 5365-5373, 2021.

35. Tandoh A, Danquah CA, Benneh CK, Adongo DW, Boakye-Gyasi E and Woode E: Effect of diclofenac and andrographolide combination on carrageenan-induced paw edema and hyperalgesia in rats. Dose Response 20: 15593258221103846, 2022.

36. Yuwen D, Mi S, Ma Y, Guo W, Xu Q, Shen Y and Shu Y: Andrographolide enhances cisplatin-mediated anticancer effects in lung cancer cells through blockade of autophagy. Anticancer Drugs 28: 967-976, 2017.

37. Mi S, Xiang G, Yuwen D, Gao J, Guo W, Wu X, Wu X, Sun Y, Su Y, Shen Y and Xu Q: Inhibition of autophagy by andro-grapholide resensitizes cisplatin-resistant non-small cell lung carcinoma cells via activation of the Akt/mTOR pathway. Toxicol Appl Pharmacol 310: 78-86, 2016.

38. Yang T, Yao S, Zhang X and Guo Y: Andrographolide inhibits growth of human T-cell acute lymphoblastic leukemia Jurkat cells by downregulation of PI3K/AKT and upregulation of p38 MAPK pathways. Drug Des Devel Ther 10: 1389-1397, 2016.

39. Kocak M, Ezazi Erdi S, Jorba G, Maestro I, Farrés J, Kirkin V, Martinez A and Pless O: Targeting autophagy in disease: Established and new strategies. Autophagy 18: 473-495, 2022.

40. Chen Y and Gibson SB: Three dimensions of autophagy in regulating tumor growth: Cell survival/death, cell proliferation, and tumor dormancy. Biochim Biophys Acta Mol Basis Dis 1867: 166265, 2021.

41. Wei H, Wang C, Croce CM and Guan JL: p62/SQSTM1 syner-gizes with autophagy for tumor growth in vivo. Genes Dev 28: 1204-1216, 2014.

42. Li X, He S and Ma B: Autophagy and autophagy-related proteins in cancer. Mol Cancer 19: 12, 2020.

43. Amaravadi RK, Kimmelman AC and Debnath J: Targeting autophagy in cancer: Recent advances and future directions. Cancer Discov 9: 1167-1181, 2019.

44. Pugsley HR: Quantifying autophagy: Measuring LC3 puncta and autolysosome formation in cells using multispectral imaging flow cytometry. Methods 112: 147-156, 2017.

45. Shi B, Ma M, Zheng Y, Pan Y and Lin X: mTOR and Beclin1: Two key autophagy-related molecules and their roles in myocardial ischemia/reperfusion injury. J Cell Physiol 234: 12562-12568, 2019.

46. Nishimura T and Tooze SA: Emerging roles of ATG proteins and membrane lipids in autophagosome formation. Cell Discov 6: 32, 2020.

47. Tran S, Fairlie WD and Lee EF: BECLIN1: Protein structure, function and regulation. Cells 10: 1522, 2021.

48. Dunn WA Jr: Autophagy and related mechanisms of lyso-some-mediated protein degradation. Trends Cell Biol 4: 139-143, 1994.

49. Gu X, Guo W, Zhao Y, Liu G, Wu J and Chang C: Deoxynivalenol-induced cytotoxicity and apoptosis in IPEC-J2 cells through the activation of autophagy by inhibiting PI3K-AKT-mTOR signaling pathway. ACS Omega 4: 18478-18486, 2019.

50. Song G, Lu H, Chen F, Wang Y, Fan W, Shao W, Lu H and Lin B: Tetrahydrocurcumin-induced autophagy via suppression of PI3K/Akt/mTOR in non-small cell lung carcinoma cells. Mol Med Rep 17: 5964-5969, 2018.

51. Fattahi S, Amjadi-Moheb F, Tabaripour R, Ashrafi GH and Akhavan-Niaki H: PI3K/AKT/mTOR signaling in gastric cancer: Epigenetics and beyond. Life Sci 262: 118513, 2020.

52. Xu Z, Han X, Ou D, Liu T, Li Z, Jiang G, Liu J and Zhang J: Targeting PI3K/AKT/mTOR-mediated autophagy for tumor therapy. Appl Microbiol Biotechnol 104: 575-587, 2020.

53. Li X, Zhang W, Liang L, Duan X, Deng J and Zhou Y: Natural product-derived icaritin exerts anti-glioblastoma effects by positively modulating estrogen receptor β. Exp Ther Med 19: 2841-2850, 2020.

54. Duarte D, Falcão SI, El Mehdi I, Vilas-Boas M and Vale N: Honeybee venom synergistically enhances the cytotoxic effect of CNS drugs in HT-29 colon and MCF-7 breast cancer cell lines. Pharmaceutics 14: 511, 2022.

55. Livak KJ and Schmittgen TD: Analysis of relative gene expression data using real-time quantitative PCR and the 2(-Delta Delta C(T)) method. Methods 25: 402-408, 2001.

56. Feng L, Lu CK, Wu J, Chan LL and Yue J: Identification of anhydrodebromoaplysiatoxin as a dichotomic autophagy inhibitor. Mar Drugs 21: 46, 2023.

57. Pierro J, Hogan LE, Bhatla T and Carroll WL: New targeted therapies for relapsed pediatric acute lymphoblastic leukemia. Expert Rev Anticancer Ther 17: 725-736, 2017.

58. Habiel DM, Krepostman N, Lilly M, Cavassani K, Coelho AL, Shibata T, Elenitoba-Johnson K and Hogaboam CM: Senescent stromal cell-induced divergence and therapeutic resistance in T cell acute lymphoblastic leukemia/lymphoma. Oncotarget 7: 83514-83529, 2016.

59. Rose-James A, Shiji R, Kusumakumary P, Nair M, George SK and Sreelekha TT: Profiling gene mutations, translocations, and multidrug resistance in pediatric acute lymphoblastic leukemia: A step forward to personalizing medicine. Med Oncol 33: 98, 2016.

60. Palmer AC, Chidley C and Sorger PK: A curative combination cancer therapy achieves high fractional cell killing through low cross-resistance and drug additivity. Elife 8: e50036, 2019.

61. Jaaks P, Coker EA, Vis DJ, Edwards O, Carpenter EF, Leto SM, Dwane L, Sassi F, Lightfoot H, Barthorpe S, et al: Effective drug combinations in breast, colon and pancreatic cancer cells. Nature 603: 166-173, 2022.

62. Pemovska T, Bigenzahn JW and Superti-Furga G: Recent advances in combinatorial drug screening and synergy scoring. Curr Opin Pharmacol 42: 102-110, 2018.

63. Li YJ, Lei YH, Yao N, Wang CR, Hu N, Ye WC, Zhang DM and Chen ZS: Autophagy and multidrug resistance in cancer. Chin J Cancer 36: 52, 2017.

64. Sarang Z, Gyurina K, Scholtz B, Kiss C and Szegedi I: Altered expression of autophagy-related genes might contribute to glucocorticoid resistance in precursor B-cell-type acute lymphoblastic leukemia. Eur J Haematol 97: 453-460, 2016.

65. Li Y, Qu M, Xing F, Li H, Cheng D, Xing N and Zhang W: The protective mechanism of dexmedetomidine in regulating Atg14L-Beclin1-Vps34 complex against myocardial ischemia-reperfusion injury. J Cardiovasc Transl Res 14: 1063-1074, 2021.

66. Wu S, He Y, Qiu X, Yang W, Liu W, Li X, Li Y, Shen HM, Wang R, Yue Z and Zhao Y: Targeting the potent Beclin 1-UVRAG coiled-coil interaction with designed peptides enhances autophagy and endolysosomal trafficking. Proc Natl Acad Sci USA 115: E5669-E5678, 2018.

67. Wu W, Wang X, Sun Y, Berleth N, Deitersen J, Schlutermann D, Stuhldreier F, Wallot-Hieke N, José Mendiburo M, Cox J, et al: TNF-induced necroptosis initiates early autophagy events via RIPK3-dependent AMPK activation, but inhibits late autophagy. Autophagy 17: 3992-4009, 2021.

68. Nakahira K, Pabon Porras MA and Choi AM: Autophagy in pulmonary diseases. Am J Respir Crit Care Med 194: 1196-1207, 2016.

69. Wesch N, Kirkin V and Rogov VV: Atg8-family proteins-structural features and molecular interactions in autophagy and beyond. Cells 9: 2008, 2020.

70. Prieto-Domínguez N, Ordóñez R, Fernández A, García-Palomo A, Muntané J, González-Gallego J and Mauriz JL: Modulation of autophagy by sorafenib: Effects on treatment response. Front Pharmacol 7: 151, 2016.

71. Yang G, Li Z, Dong L and Zhou F: lncRNA ADAMTS9-AS1 promotes bladder cancer cell invasion, migration, and inhibits apoptosis and autophagy through PI3K/AKT/mTOR signaling pathway. Int J Biochem Cell Biol 140: 106069, 2021.

72. Petrulea MS, Plantinga TS, Smit JW, Georgescu CE and Netea-Maier RT: PI3K/Akt/mTOR: A promising therapeutic target for non-medullary thyroid carcinoma. Cancer Treat Rev 41: 707-713, 2015.